Journal of
Iberian Geology
AN INTERNATIONAL PUBLICATION OF EARTH SCIENCES

Facies heterogeneity of a Kimmeridgian carbonate ramp (Jabaloyas, eastern Spain): a combined outcrop and 3D geomodelling analysis

Heterogeneidad de facies en una rampa carbonatada del Kimmeridgiense (Jabaloyas, Este de España): análisis de campo y geomodelización tridimensional

G. San Miguel[1]*, M. Aurell[1], B. Bádenas[1], V. Martínez[1], B. Caline[2], C. Pabian-Goyheneche[2], J.P. Rolando[2], N. Grasseau[3]

[1] University of Zaragoza, c/ Pedro Cerbuna, 12, 50009 – Zaragoza, Spain
galosanmiguel@gmail.com; maurell@unizar.es; bbadenas@unizar.es; vicmartinezgarcia@hotmail.com
[2.] Total E&P, Technology Centre, CSTJF, Avenue Larribau, F-64018 Pau Cedex, France
bruno.caline@total.com; cecile.pabian-goyheneche@total.com; jean-paul.rolando@total.com
[3] EGID, University of Bordeaux, 3 – 1. 33607 Pessac Cedex - France
nicolas.grasseau@free.fr

*corresponding author

Abstract

The Upper Kimmeridgian outcrops exposed around the village of Jabaloyas (NE Spain) have been analyzed to document the facies heterogeneity across the shallow portion of a low angle carbonate ramp. The studied area covers a total surface of 12 square kilometres. Seventeen stratigraphic profiles have provided basic information to carry out the detailed facies analyses presented in this work. The studied unit corresponds to a high-frequency sequence, bounded by discontinuities that can be traced at regional scale. This sequence shows the widespread development of coral-microbial reef buildups with conical to cylindrical shape (up to 19 m thick).

The characterization and interpretation of the different sort of inter-reef and post-reef facies resulted in the reconstruction of the sedimentary domains of the studied carbonate ramp, from burrowed mud-dominated skeletal facies (distal middle ramp), to grainy (skeletal, peloidal, oolitic) shoal and backshoal facies (inner ramp). The studied sequence is divided into four sedimentary episodes bounded by sharp facies changes. The lower two episodes include the vertical reef growth during rapid accommodation gain; the upper two episodes are marked by the rapid progradation of the inner ramp facies.

The depositional facies and their stacking patterns in the Jabaloyas outcrops are similar to those described in the subsurface Arab D reservoirs. This Late Jurassic carbonate unit forms major hydrocarbon fields in the Middle East. For improving the geological distribution of reservoir heterogeneity in this kind of low angle carbonate ramp system, two 3D models have been created. A Full-field Model of the overall geometry of the facies belts has allowed the quantification of vertical and lateral extension of the inter-reef and post-reef facies. A Sector Model, which includes individual reef bodies has been used to better simulate reservoir heterogeneity resulting from different diagenetic overprint.

Keywords: carbonate ramp, Upper Jurassic, reefs, 3D modelling, Iberian Basin.

Resumen

Los afloramientos del Kimmeridgiense Superior en las cercanías de Jabaloyas (NE de España) han sido estudiados para documentar la heterogeneidad de facies en las zonas más someras de una rampa carbonatada de bajo ángulo. El área de estudio cubre una superficie de 12 kilómetros cuadrados en la que se han levantado diecisiete columnas estratigráficas y se ha realizado un análisis detallado de facies. La unidad estratigráfica estudiada corresponde a una secuencia de alta frecuencia limitada por discontinuidades que pueden ser cartografiadas a escala regional. Dicha secuencia presenta bioconstrucciones arrecifales coralinas y microbianas con morfologías cónicas o cilíndricas de hasta 19 m de potencia.

La caracterización e interpretación de las diferentes facies inter- y post-arrecifales ha permitido la reconstrucción de los diferentes dominios de la rampa carbonatada, desde facies no granosostenidas bioturbadas (rampa media distal), hasta facies granosostenidas (bioclásticas, peloidales, oolíticas) desarrolladas en bajíos activos y en zonas someras protegidas. La existencia de superficies bien cementadas y de cambios abruptos de facies asociados ha permitido la división de la secuencia en cuatro episodios de sedimentación. Los dos primeros incluyen el crecimiento de los arrecifes durante los periodos de ganancia de acomodación, mientras que los dos últimos vienen marcados por una rápida progradación de las facies de rampa interna.

El patrón de apilamiento de esta unidad en los afloramientos de Jabaloyas muestra similitudes con aquellos descritos en los reservorios desarrollados en el Arab D, el cual genera campos de hidrocarburos de gran tamaño en Medio Oriente. Con el fin de precisar la heterogeneidad de facies a escala de reservorio en este tipo de rampas carbonatadas de bajo ángulo, se han elaborado dos modelos tridimensionales. Un modelo de campo completo ha permitido precisar la extensión y la geometría de los diferentes cinturones de facies; y un modelo sector, que incluye los cuerpos arrecifales, posteriormente utilizado para simular la heterogeneidad del reservorio con ayuda de estudios diagenéticos previos.

Palabras clave: rampa carbonatada, Jurásico Superior, arrecifes, modelización 3D, Cuenca Ibérica

1. Introduction

Carbonate reservoirs from the Middle East are the most important hydrocarbon sources worldwide (BP Statistical Review, 2011). Among these hydrocarbon fields, some are reaching a mature stage where internal heterogeneity needs to be understood in order to optimize ultimate recovery (Enhance Oil Recovery -EOR- and Improved Oil Recovery -IOR- phases). The Upper Jurassic Arab D reservoirs are one example of these heterogeneous carbonate reservoirs. This work is focussed on the Upper Kimmeridgian carbonate strata which are well exposed in outcrops around the Jabaloyas village (Northeast Spain; Fig. 1). The Jabaloyas deposits share similarities with the Arab D carbonates in terms of age, lithofacies and depositional environments and could represent a valuable outcrop analogue.

The main purpose of this work is the characterization of the vertical and lateral facies distribution of the Upper Kimmeridgian strata in Jabaloyas outcrop with the main target of constraining the spatial distribution of carbonate lithofacies types and the sedimentary heterogeneity of the Arab D reservoirs. The use of outcrops has become one of the most important tools for documenting the heterogeneities at various scales (Jahn *et al*., 2003; Jennings, 2000) thanks to the continuous exposures in both vertical and horizontal directions. The examination of outcrop analogues provides a better understanding of the fine scale reservoir heterogeneity, as required for EOR of many mature oil fields in Arab D carbonates.

The Arab D deposits were accumulated in the southern realm of the Tethys. This unit mostly consists of well-sorted oolitic packstone-grainstone forming active shoals and patch reefs mainly composed by stromatoporoids in the foreshoal environment (Gröstch *et al*., 2003). As the studied analogue of Jabaloyas, the Arab D deposits occurred in the shallow domains of an Upper Kimmeridgian carbonate ramp (Ayoub and En Nadi, 2000; Al-Saad and Ibrahim, 2005). However, a significant difference with the studied strata around Jabaloyas is the presence of interbedded evaporitic deposits, observed to be episodically deposited in the supratidal environments of the Arab D reservoir. The quality of this reservoir is due to the interparticle porosity in the peloidal and oolitic grainstones and the vuggy porosity resulting from the dissolution of stromatoporoids bioclasts. Consequently, it is crucial to reproduce the distribution of shoals and reef bodies in the 3D reservoir model if realistic simulation of the flow units is meant to be achieved in this heterogeneous reservoir (Lehman *et al*., 2008).

The study of the facies distribution in the Jabaloyas outcrops has been primarily based on a detailed sedimentological analysis including a thorough characterization of facies, depositional architecture and sedimentary environments of the Kimmeridgian carbonate ramp. These data have been used to construct a 3D geological model, which has allowed further understanding and quantification of the field information. These well documented 3D models have contributed to better understand and quantify facies distribution in a subsurface Arab D reservoir and therefore to reduce the geological uncertainties associated with facies heterogeneities in a similar carbonate ramp reservoir.

2. Geological setting

Extensive carbonate platforms covered the eastern part of the Iberian Plate during Late Jurassic times. These carbonate ramps were open to the Tethys towards the SE-ESE (Fig. 2). The studied Kimmeridgian unit corresponds to the Torrecilla Formation, which represents the shallow facies belts of the Iberian low angle carbonate ramp. This unit includes the local development of coral-microbial reef buildups which coexisted with sediments showing a large variety of non-skeletal components such as ooids, peloids, intraclasts and oncoids. This shallow facies belt progressively graded eastwards to the slightly deeper part of the carbonate ramp where lime mudstones
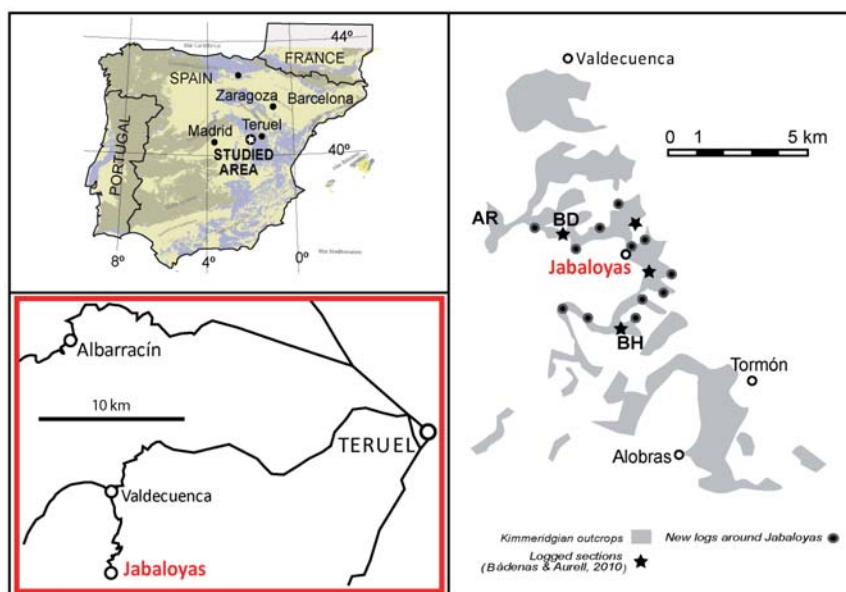

Fig. 1.- Location of Jabaloyas in NE of Spain. The extent of the Kimmerdigian outcrops at a regional scale is shown on the right sketch. The study area around Jabaloyas is squared, indicating in black circles the location of the studied stratigraphic profiles (the stars are the logs studied in Bádenas and Aurell, 2010).

Fig. 1.- Localización de Jabaloyas (Noreste de España). A la derecha, la extensión de los afloramientos del Kimmeridgiense. La zona de estudio encuadrada muestra la situación de los perfiles estratigráficos realizados (las estrellas corresponden a los perfiles estudiados en Bádenas and Aurell, 2010).
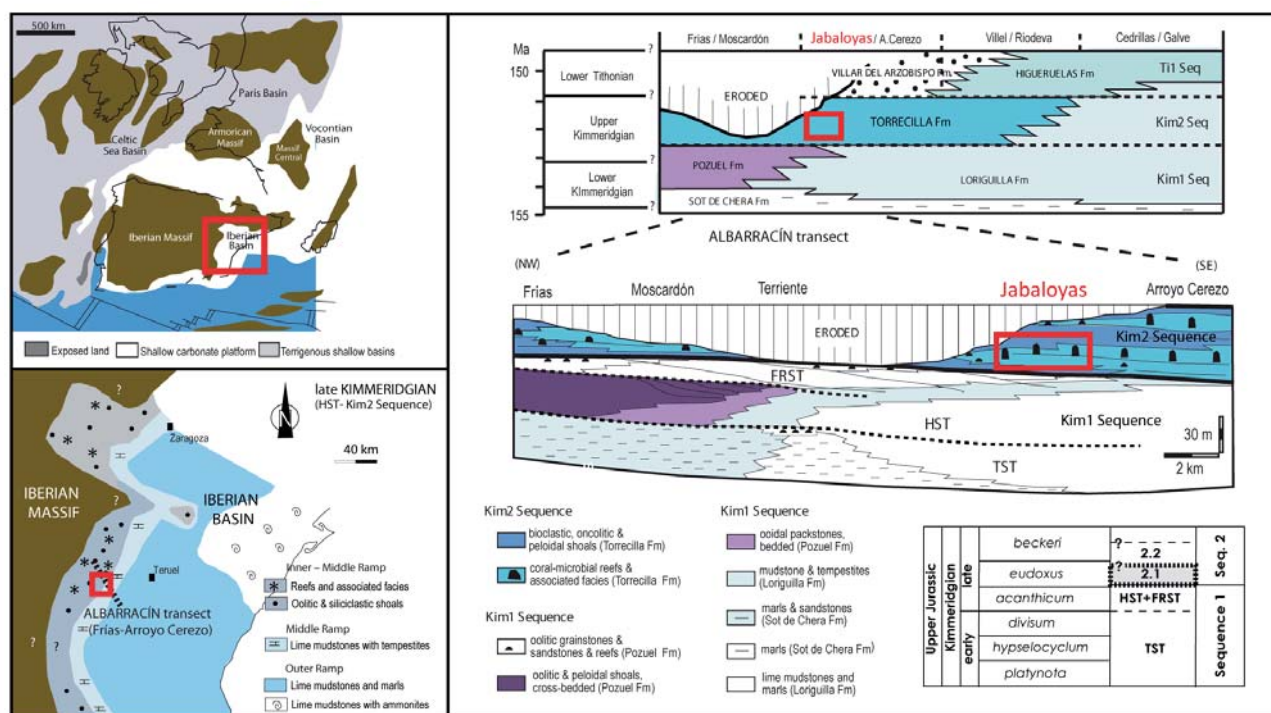

Fig. 2.- Palaeogeography, overall facies distribution and stratigraphy of the Kimmeridgian of the Iberian Basin. The studied locality (squared) corresponds to the inner to middle ramp domains within the Kimmeridgian sequence 2 (Kim2 seq, Torrecilla Formation). Compiled from Bádenas and Aurell (2010).

Fig. 2.- Paleogeografía, distribución general de facies y estratigrafía del Kimmeridgiense de la cuenca Ibérica. La localidad estudiada (ver recuadro), corresponde a dominios de rampa interna y rampa media dentro de la secuencia Kimmeridgiense-2 (Kim2 seq, Formación Torrecilla). Recopilado a partir de Bádenas and Aurell (2010).

Fig. 3.- The studied area covers 17 km of linear outcrops, where 17 detailed stratigraphic profiles were carried out (big red circles). The small green circles in the upper picture are the 274 reef build-ups that were mapped and georeferenced. Two exported pictures from Petrel software give a general view of the roundabouts of Jabaloyas where Torrecilla Fm (white colour) outcrops along the gullies, which penetrate towards Javalon Hill. The star locates the Jabaloyas village.

Fig. 3.- El afloramiento tiene una longitud lineal de 17 km, donde se levantaron 17 perfiles estratigráficos (círculos grandes). Los círculos pequeños señalan los 274 arrecifes bioconstruidos que fueron cartografiados y georeferenciados. Las dos fotografías exportadas del programa Petrel (perfil inferior) permiten una vista general del afloramiento de la Formación Torrecilla (en blanco) que se extiende por la zona de cabecera de los barrancos que rodean al Cerro Javalón. La estrella representa la situación de la localidad de Jabaloyas.

and marls accumulated (e.g., Bádenas and Aurell, 2001; Aurell and Bádenas, 2004).

The Torrecilla Formation forms part of a third-order sequence (i.e., Kim 2 Sequence), which was mostly developed during the Late Kimmeridgian (e.g., Bádenas and Aurell, 2001; Aurell *et al*., 2003; see Fig. 2). This age assignment is based on the scarce ammonite and mi-

crofossil content (i.e., benthic foraminifera, calcareous algae; e.g., Fezer, 1988; Nose, 1995; Bádenas and Aurell, 2001). Around Jabaloyas, the Upper Kimmeridgian Torrecilla Formation consists of five high-frequency sequences bounded by regional discontinuities, which were tentatively related to sea level fluctuations controlled by orbital cycles (high-frequency Sequences A to E in Báde-
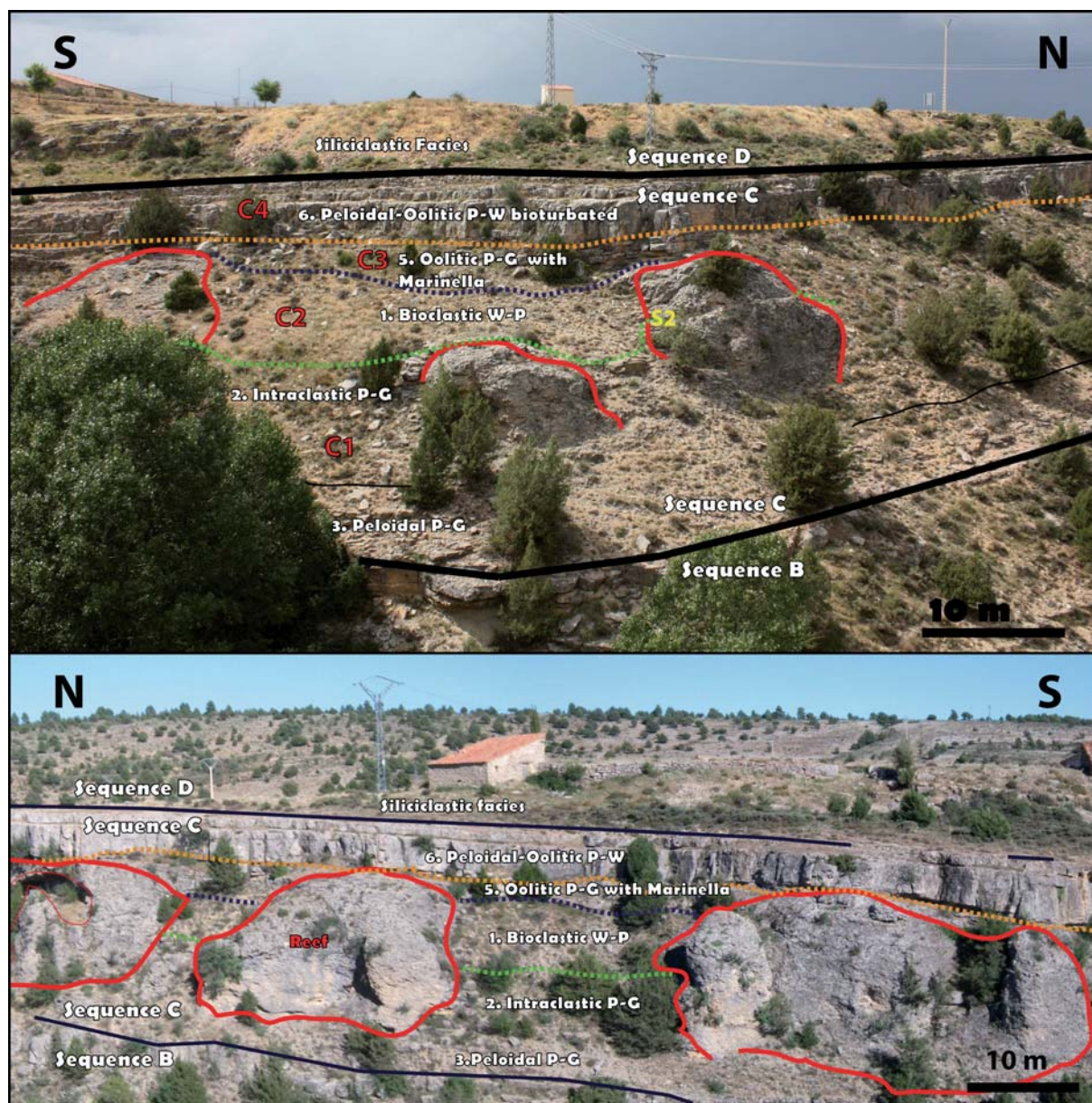
Fig. 4.- Field pictures from Barranco de la Canaleja (BC2: upper picture; BC3: lower picture) showing the distribution of the different facies types and their relationship to the coral-microbial buildups in a relatively distal mid-ramp locality.

Fig. 4.- Fotografías del afloramiento del Barranco de la Canaleja (BC2: fotografía superior; BC3: fotografía inferior). Se indica la distribución de los tipos de facies diferenciados y su relación con los arrecifes coralinos y microbianos en una zona distal de rampa media.

nas and Aurell, 2010). The present work concentrates on the high-frequency Sequence C, which shows a variable thickness across the study area from 12 to 20 m. This sequence includes the largest development of coral-microbial reef buildups found around the Jabaloyas area.

3. Methodology

The outcrops of the Torrecilla Formation studied around the Jabaloyas village are squared in the left part of figure 1. Fieldwork included the logging of 17 detailed sedimentological profiles, the geological mapping of the facies using photomosaics of the intermediate areas, and the georeferencing and detailed documentation of 274 reef buildups along the studied outcrop (Fig. 3). All data were georeferenced over the Digital Elevation Model (DEM, 1:5000) in combination with the aerial photos (50 cm pixel resolution) from the Geographic Information System webpage of the Aragon Government.

Around 160 samples were collected to complete the facies description under binocular and petrographic microscope. Petrographic analysis allowed determining the semiquantitative proportion of skeletal and non-skeletal components (visual estimation with petrographical tem-
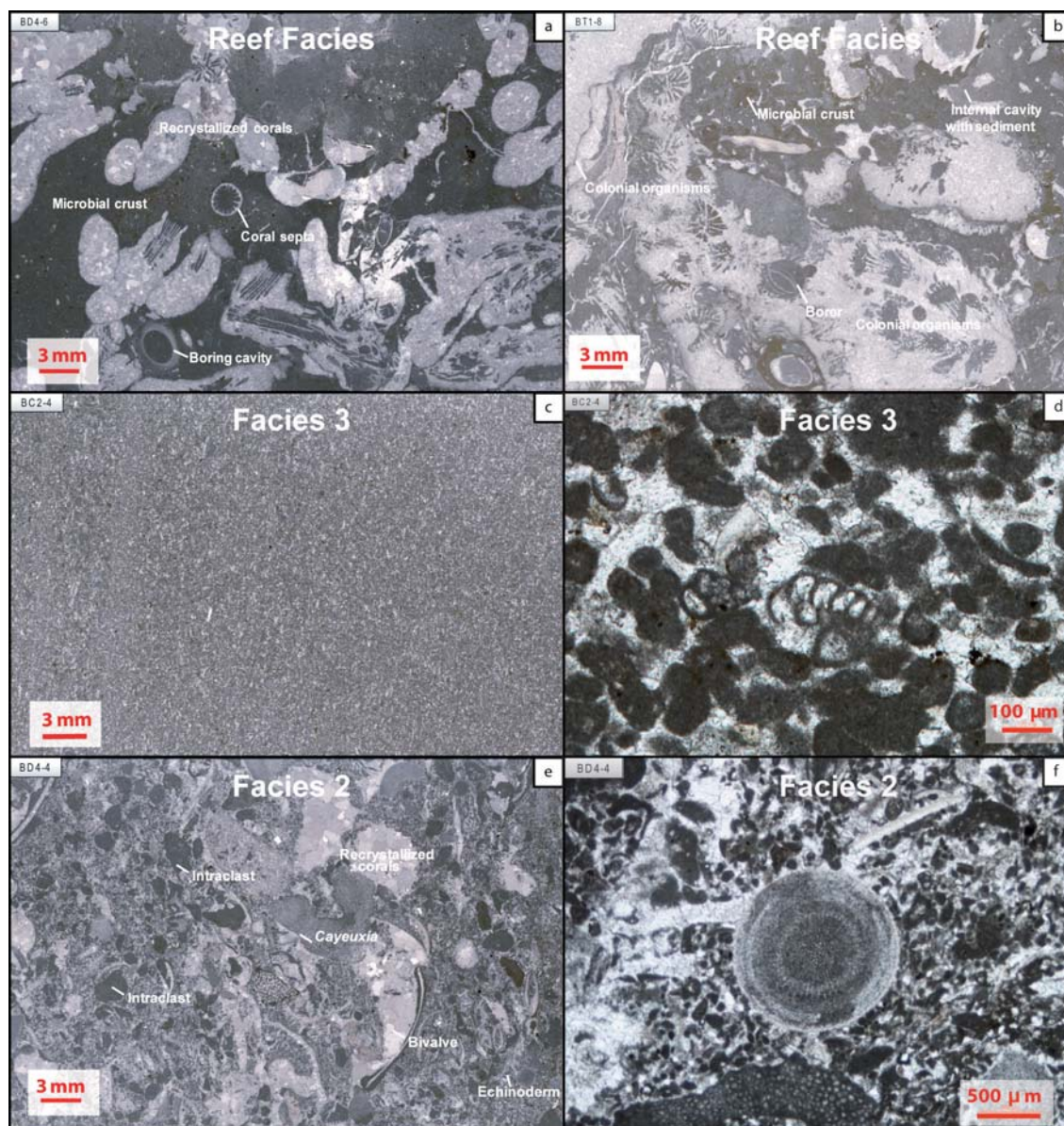
Fig. 5.- Thin sections showing the main characteristics of each facies: a) reef facies with bioclasts of colonial organisms such as corals, stromatoporoids and algae; the microbial crust is represented by darker zones and some cavities that were early filled by internal sediment; b) reef facies: coral bioclasts totally recrystallized are surrounded by microbial crust; c) facies 3: peloidal packstone-grainstone very well sorted and peloids represent nearly 100% of the components; d) facies 3: angular to rounded peloids that show similar origin to intraclast derived from microbial crust; e) facies 2: poorly sorted facies, including large amount of reef derived intraclasts, such as clasts from the microbial crust and bioclasts of colonial organisms, as well as echinoderms, bivalves and algae; f) facies 2: spike of echinoderm surrounded mainly by intraclasts, algae and peloids.

Fig. 5.- Láminas delgadas mostrando las características principales de cada facies: a) facies arrecifal (con bioclastos de organismos coloniales como corales, estromatopóridos y algas); la costra microbial caracterizada por las zonas oscuras y las cavidades que fueron rellenadas por sedimento interno en una etapa temprana; b) facies arrecifal: bioclastos de coral totalmente recristalizados rodeados por costra microbiana; c) facies 3: packstone-grainstone peloidal bien clasificada mostrando una proporción de peloides cerca del 100% de los componentes; d) facies 3 : peloides angulares y redondeados que muestran un origen similar al de los intraclastos, todos ellos derivados de la costra microbial de los arrecifes; e) facies 2: clasificación mala, incluye grandes proporciones de intraclastos provenientes de la masa arrecifal (clastos de costra microbial, corales, así como fragmentos de equinodermos, bivalvos y algas); f) facies 2: espícula de equinodermo rodeada mayoritariamente de intraclastos, algas y peloides.

plates) as well as texture following Dunham (1962) and Embry and Klovan (1971) classifications. For the description of coated grains, the proposed nomenclature for oncoids (Dahanayake, 1977, 1978) and ooids (Strasser, 1986) was adopted. Cathodoluminescence tests were carried out over some thin sections. The results showed low luminescence in all the studied thin sections.

A number of facies types were differentiated and interpreted, in order to reconstruct the different sedimentary environments across the studied carbonate ramp. Lateral
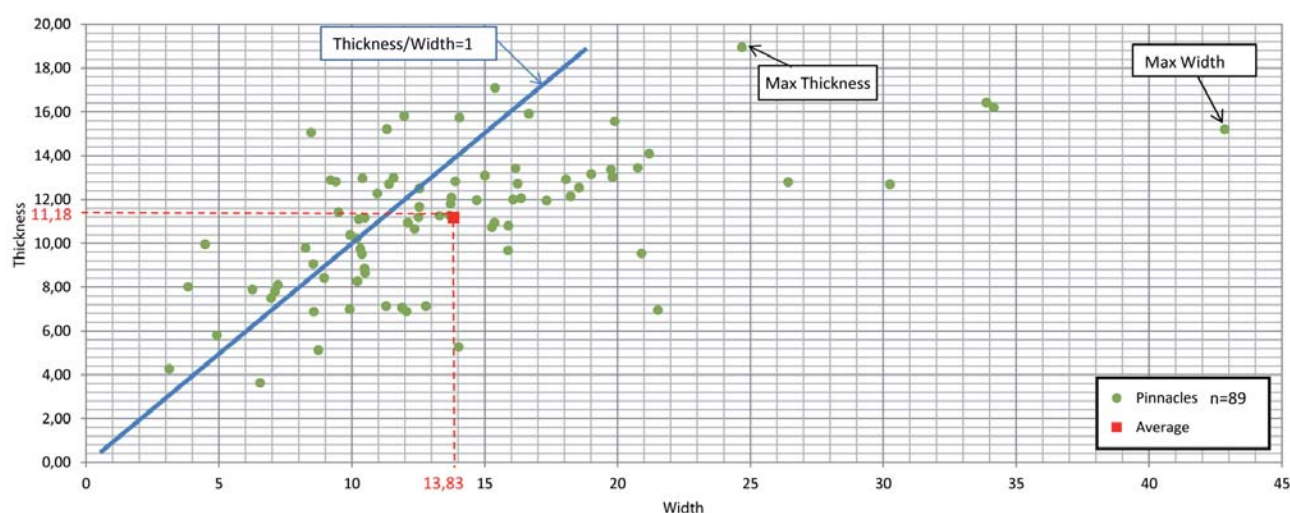
Fig. 6.- 89 reef bodies (points) were measured along the studied area. The height and width of each body is reported and compared with the line 1:1 (straight diagonal line). These buildups show conical to cylindrical pinnacle geometry up to 19 m in thickness and 43 m in width.

Fig. 6.- 89 cuerpos arrecifales (puntos) fueron medidos a lo largo de la zona de estudio. La altura y la anchura de dichos cuerpos se ven expuestas comparándolas con la línea de proporción 1:1 (línea diagonal). Muestran morfologías cónicas y cilíndricas de pináculo hasta 19 m de potencia, alcanzando los 43 de ancho.

and vertical facies trends are shown by different cross-sections. Sequence analysis was performed on the recognition of stacking patterns in the facies successions. Sharp facies changes associated with prominent surfaces have been considered as time-lines at outcrop-scale, and have been used to subdivide the studied high-frequency C into four sedimentary episodes.

This set of stratigraphic and sedimentological data forms the basis for the reconstruction of the 3D outcrop model. The vertical and lateral facies distribution reconstructed from fieldwork was modelled by using Petrel 2010.2 E&P Software Platform® (Schlumberger Limited, 2011). Two 3D models were built. The complete modelling of the study area around Jabaloyas or Full-field Model had a grid increment of 20 x 20 m. This grid increment is suitable to show the overall distribution of the different inter- and post-reef facies but does not give enough resolution to include the coral-microbial reefs, because the cell size is bigger than most of the documented buildups. The cemented bed found at the top of the studied interval, which is a prominent cemented surface, traceable across the study area, was used for mapping, georeferencing and reconstructing in 3D the Sequence C along the gullies. A more specific area was modelled (i.e., the Sector Model) in order to define precisely the relationship between the coral-microbial reefs and the inter-reef facies.

4. Facies types

Nine facies types have been distinguished based on main components, texture and sedimentary structures. They have been grouped in three facies associations: coral-microbial reef facies, inter-reef facies, and post-

reef facies. Inter-reef facies 1 to 5 and post-reef facies 6 to 8 are numbered according to the distal-proximal relationship (i.e., from the relatively distal facies 1 to the proximal lagoonal facies 7 and 8). The description and interpretation of each facies type is provided below. Figure 4 illustrates two examples of facies distribution from field photomosaics.

4.1. Coral-microbial reef facies

The reef fabric basically consists of boundstones with variable proportion of colonial organisms (up to 90% of the components), microbial crusts and associated encrusting organisms (10-80%), and cavities filled by internal sediment (Fig. 5a,b). The observed proportion of colonial organisms and microbial crusts allowed to define two types of fabrics (Aurell and Bádenas, 2004) according to the classification of Leinfelder (1993): coral-microbial reefs (colonial organisms forming the largest proportion of the fabric); and coral-bearing thrombolites (colonial organisms and microbial crust found in similar proportion). The most common coral genera are *Thamnasteria, Cosmoseris* and *Microsolena. Calamophylliopsis, Stylina excelsa, Ovalastrea delgadoi, Milleporidium formosum, Axosmilia infundibuliformis, Ovalastrea delgadoi* occur in lower proportion (Fezer, 1988; Nose, 1995). Stromatoporoids, chaetetids, sponges, *Solenopora sp.*, bivalves and echinoderms are also present. The microbial crust shows dense micritic and micro-peloidal fabric, and associated encrusting organisms (serpulids, bryozoans, *Koskinobullina, Lithocodium, Tubiphytes, Bacinella* and solenoporacean algae). Most of the internal cavities were early filled by either mud- or grain-supported sediment
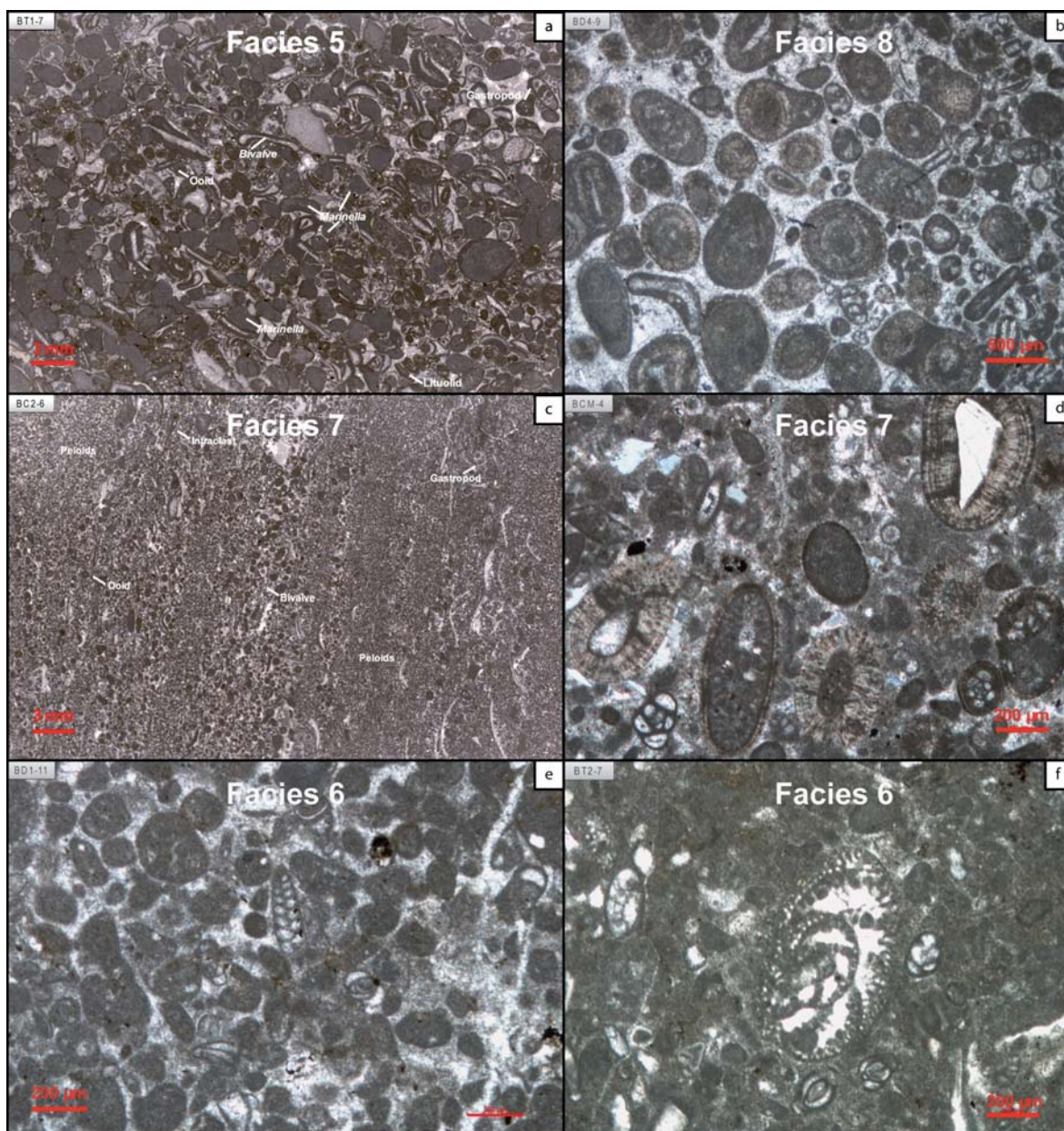
Fig. 7.- (a) Facies 5, dominated by bioclasts from the red algae *Marinella lugeoni*; (b) facies 8: sparitic ooids reaching almost 100% of the components; (c) facies 7: lamination formed by alternation of peloids and coarser bioclastic-intraclastic levels; (d) facies 7: benthic foraminifera (lituolids, miliolids) and gastropods, some of them found as nuclei of the sparitic-micritic ooids; (e) facies 6: peloids, benthic forams and low proportion of micritic matrix; (f) facies 6: *Alveosepta jaccardi* is one of the most abundant lituolid in this ramp domain.

Fig. 7.- a) Facies 5: predominan los bioclastos de la alga roja *Marinella lugeoni*; b) facies 8: ooides esparíticos alcanzando una proporción de 100% de los componentes; c) facies 7: laminación formada por la alternancia niveles ricos en peloides y otros de bioclastos y de intraclastos; d) facies 7: foraminíferos bentónicos (lituólidos, miliólidos) y gasterópodos, algunos de ellos formando los núcleos de los ooides esparíticos y micríticos; e) facies 6: peloides, foraminíferos bentónicos y, en menor proporción, matriz micrítica; f) facies 6: *Alveosepta jaccardi* es una de los más abundantes entre los lituólidos encontrados en este dominio de la rampa.

derived from inter-reef sediments described below. Geopetal fillings are also common.

The coral-microbial reefs form isolated buildups that have vertical to sub-vertical walls, with variable size across the studied area, between 4–19 m in thickness and 3–43 m in width. Some trends have been found from proximal (N) to distal (S-SE) localities. Most of them rely in the 1:1 line if the relationship between their height and width is plotted (Fig. 6). However, they can be amalgamated, forming "ribbons" up to 50 m long in more proximal domains (i.e., close to BD1 section, see Fig. 3), while they form pinnacle cylindrical buildups in distal areas where they tend to grow more vertically than laterally. The average linear distance between buildups is 50 m. Nevertheless, as a general rule, buildup density increases progressively towards proximal localities.

Fig. 8.- Field pictures summarizing some geometries and sedimentary structures: (a) mud-supported facies 1 onlapping the coral-microbial buildup; (b) *Planolites*, facies 3; (c) cross-bedding, facies 4; (d) hummocky type cross-stratification, facies 4; (e) planar cross-stratification, facies 8; (f) facies 5 onlapping the coral-microbial buildup.

Fig. 8.- Fotografías de campo ilustrando las geometrías y estructuras sedimentarias: a) facies 1 no granosostenidas onlapando los arrecifes coralinos; b) *Planolites*, facies 3; c) estratificación cruzada, facies 4; d) estratificación cruzada tipo hummocky, facies 4; e) estratificación cruzada planar, facies 8; f) facies 5 con geometría de onlap sobre la parte superior de los arrecifes coralinos y microbiales.

The buildups may locally occur as metre-decimetre scale laterally continuous patches (i.e., biostromes), dominated by branching corals in growth position and large stromatoporoids (i.e., decimetre-size). This particular type of coral-stromatoporoid reef has been found in proximal areas with some degree of temperature and salinity fluctuations (C3 episode, see below). The increasing proportion of stromatoporoids towards the proximal

domains of the ramp (compared to corals) agrees with previous observations and models for the NW Tethyan realm (e.g., Leinfelder *et al*., 2005; Aurell *et al*., 2011).

4.2. Facies 1: Burrowed bioclastic mudstone-wackestone

The facies is formed by tabular to irregular (nodular) limestone beds (up to 0.4 m thick), interbedded with cen-
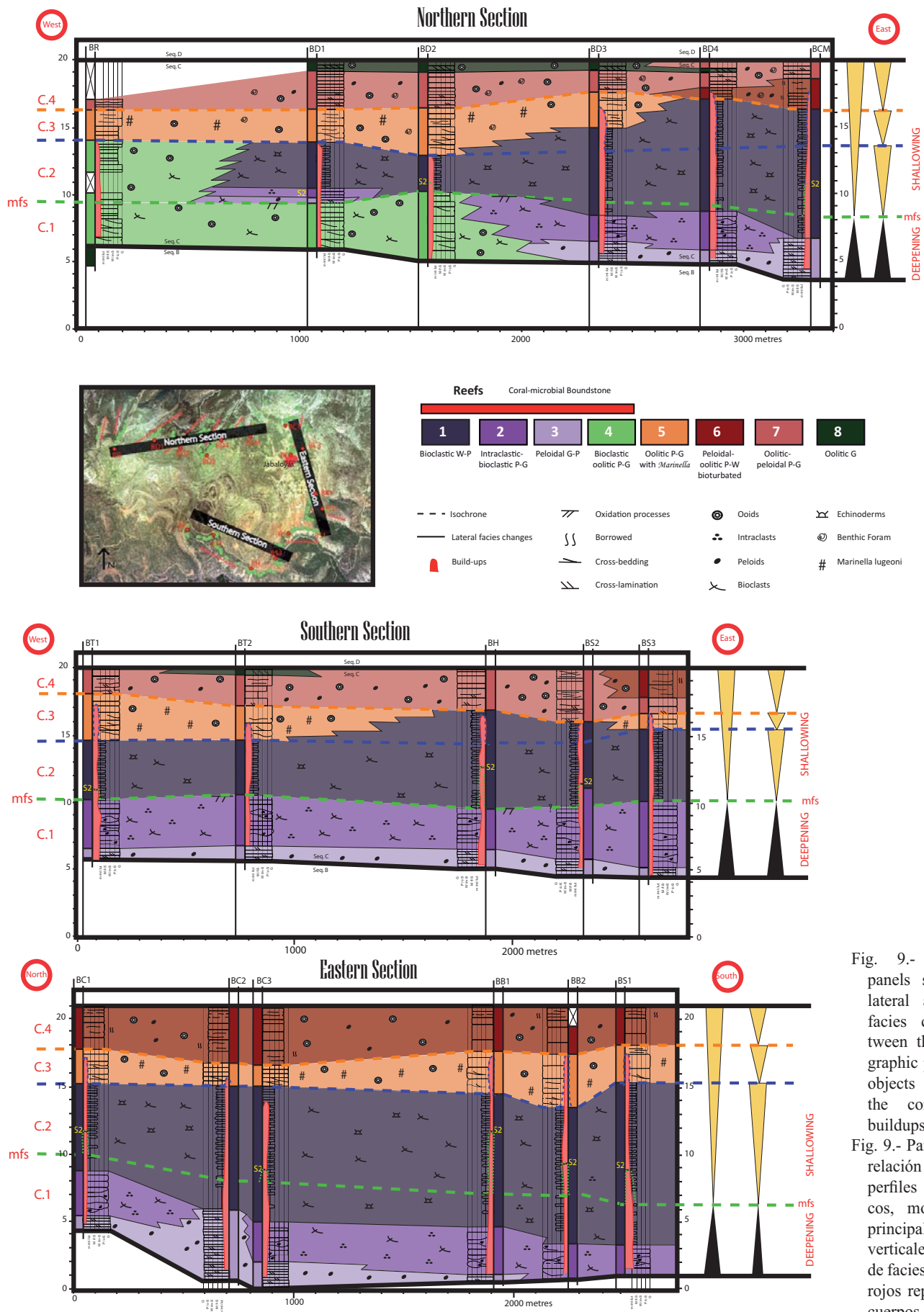
Fig. 9.- Correlation panels showing the lateral and vertical facies changes between the 17 stratigraphic profiles. Red objects represent the coral-microbial buildups.

Fig. 9.- Paneles de correlación de los 17 perfiles estratigráficos, mostrando los principales cambios verticales y laterales de facies. Los objetos rojos representan los cuerpos arrecifales.

timetre- to decimetre-thick marls (Fig. 8a). Cemented beds richer in large-size bioclasts are also found forming "aprons" around the reefs (coarser textures surrounding the buildups, i.e., rudstone and floatstone). The dominant bioclasts are bivalves (including ostreids), echinoderms (up to centimetre-size) and corals. Less common are gastropods, solenoporacean algae, chaetetids and foraminifera (lituolids). Irregular and poorly rounded peloids and intraclasts mostly corresponding to small-size debris of microbial crusts may occasionally represent up to 70% of the components.

The high proportion of lime mud and clay (i.e., marls) indicates the low-energy more distal environment of the studied ramp sector. The thickness of this facies varies from 3 m in proximal areas to 14 m in distal ones, and it indicates that deeper depositional setting occurred towards the SE.

4.3. Facies 2: Intraclastic-bioclastic packstone-grainstone

The facies consists of tabular to irregular beds (up to 0.4 m thick) with frequent hummocky cross-stratification and cross-bedding (Fig. 8c,d). Burrowed bedding surfaces are frequently found. Reef-derived intraclasts dominate (up to 90% of the components). They are up to 5 mm in diameter and mostly correspond to fragments of microbial crusts and reworked micrite (Fig. 5e,f). Peloids are also common and may form in some cases up to 50% of the components. The bioclasts (up to 70% of the compo-

nents) are bivalves, foraminifera (lituolids), echinoderms and serpulids. Less frequent are corals, gastropods, solenoporacean, *Cayeuxia* and miliolids. Type I oncoids are present in low proportion.

The grain-supported textures point to a more energetic and proximal environment compared to muddy facies 1. Hummocky cross-stratification indicates storm-induced flows probably below the fair-weather base level.

4.4. Facies 3: Peloidal grainstone-packstone

The facies is characterized by tabular to irregular beds (up to 0.5 m thick) with frequent cross-lamination and local hummocky and planar cross-bedding. *Thalassinoides* traces are usually found (Fig. 8b) and *Planolites* traces are also common. The peloids usually form up to 90% of the components (Fig. 5c,d). They are ovoid and irregular in shape, and up to 0.2 mm in mean diameter (up to 0.4 mm occasionally). Most of them correspond to small size-irregular, well-sorted and poorly rounded lithic peloids (according to Flügel, 2004), with similar origin to the boundstone-derived intraclasts described in facies 2 (Fig. 5d). The bioclasts (up to 20% of the components) consists of bivalves, echinoderms and foraminifera (lituolids, miliolids and textularids). Less common are gastropods and corals. Type 1 ooids may be locally present (up to 20% of the components). They are ovoid and spherical in shape and up to 0.7 mm in diameter.
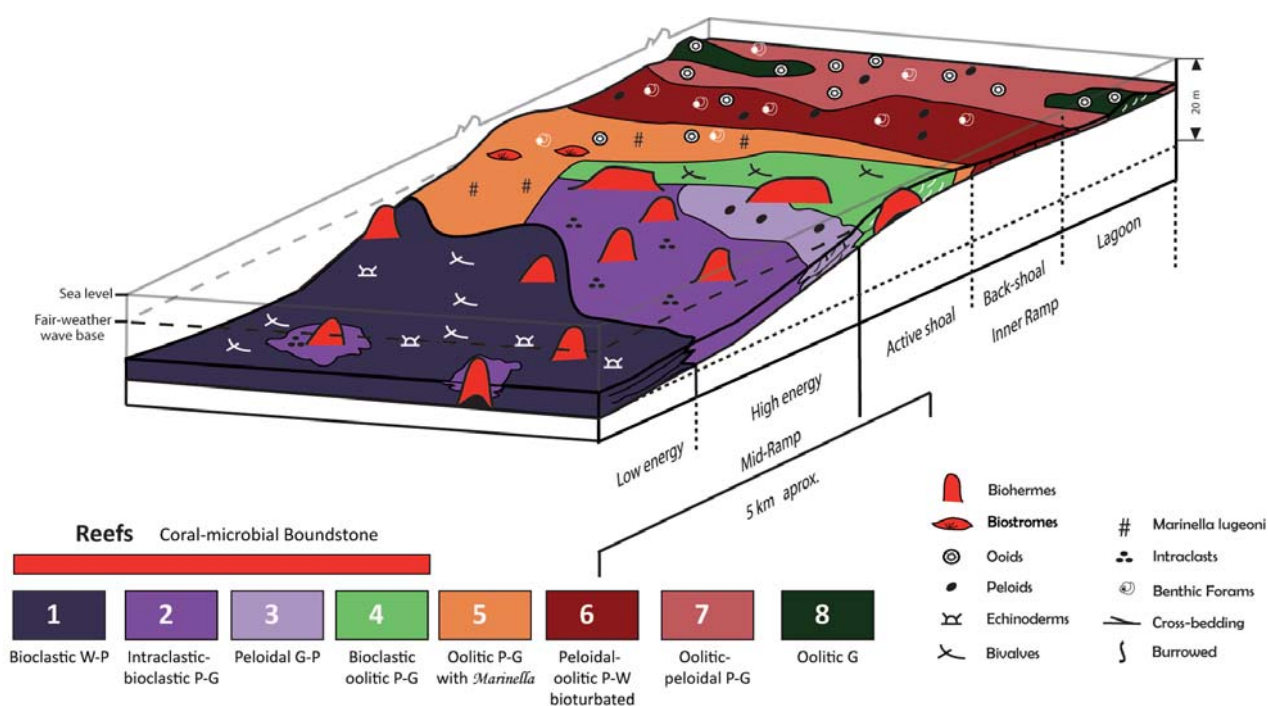

Fig. 10.- Sedimentological model, showing the facies distribution across the Upper Kimmeridgian carbonate ramp in the Jabaloyas area.

Fig. 10.- Modelo sedimentario y su correspondiente distribución de facies para la rampa carbonatada del Kimmeridgiense Superior en los alrededores de Jabaloyas.
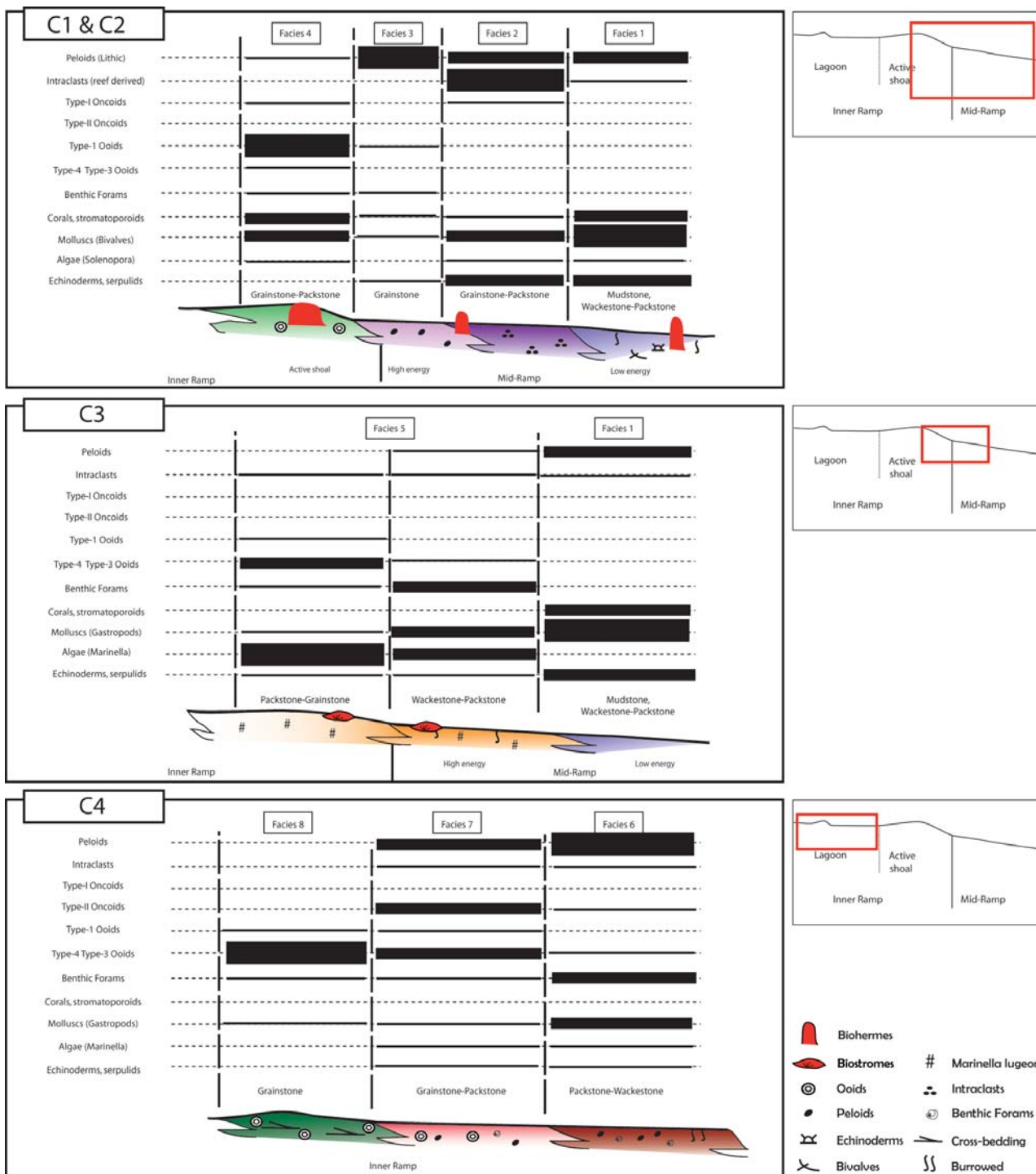
Fig. 11.- Semiquantitative analysis of the carbonate components for each episode. The sketch on the right provides the sedimentary context within the ramp. The thickness of the thick black lines increases according to the proportion of the component. The reef buildups are presented exclusively in C1 and C2 episodes.

Fig. 11.- Análisis semicuantitativo de los componentes carbonatados para cada estadio evolutivo. El esquema de la derecha ofrece la situación dentro de la rampa. El espesor de las líneas negras gruesas incrementa de acuerdo con su proporción relativa. Los arrecifes solo se desarrollan en los estadios C1 y C2.

The cross-laminated, well-sorted fine-grained facies would correspond to isolated bars migrating in the mid-ramp area. The common presence of burrowed intervals indicates frequent sedimentary interruptions in mid-ramp domains.

4.5. *Facies 4: Bioclastic-oolitic packstone-grainstone*

This facies is arranged in tabular to irregular beds (up to 0.3 m thick) with local planar cross-bedding and chan-nelized bases. Skeletal grains (up to 70% of the compo-

Fig. 12.- Successive facies maps re-
constructed for the four episodes
identified within the studied high-
frequency Sequence C.

Fig. 12.- Mapas de facies reconstrui-
dos para cada estadio evolutivo di-
ferenciado dentro de la secuencia de
alta frecuencia C.
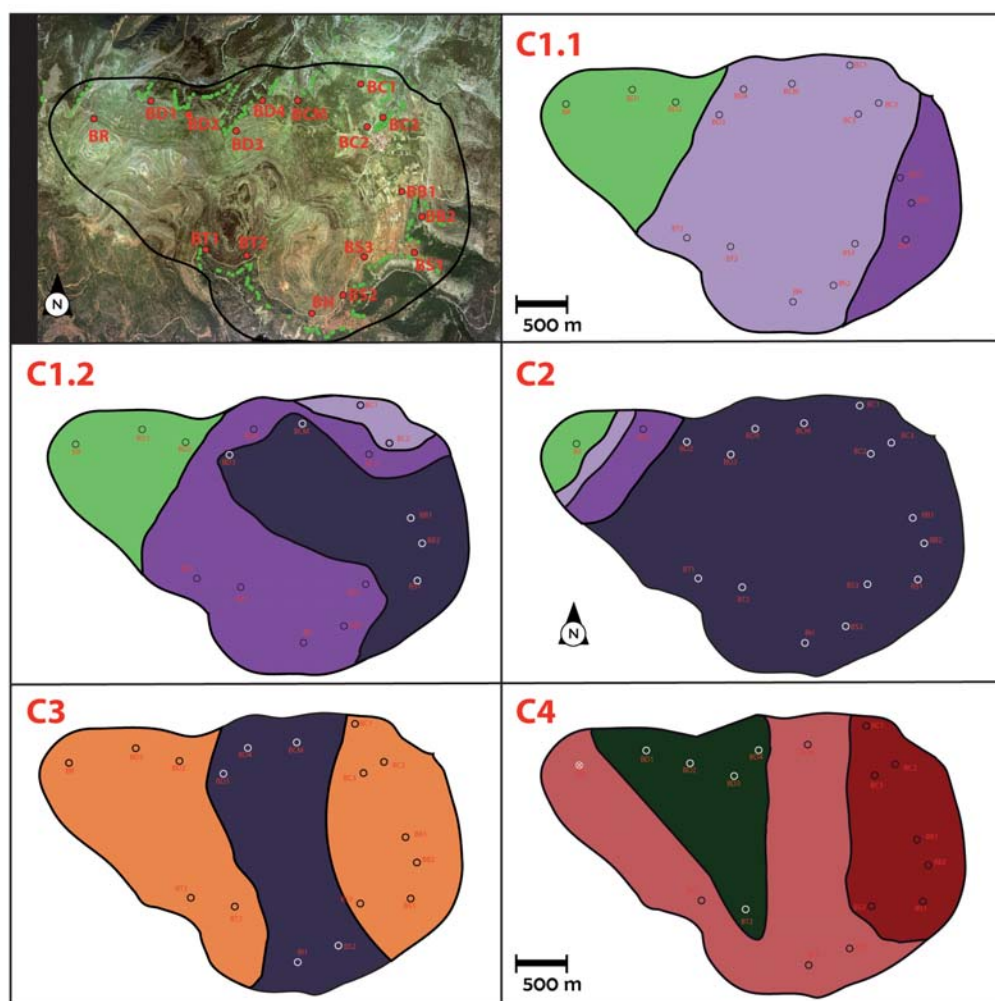
nents) mainly correspond to bivalves, corals, solenopo-
racean and chaetetids. Less common are echinoderms,
foraminifera (lituolids), gastropods and dasycladacean
algae. Type 1 ooids (up to 1 mm in diameter) may form
up to 60% of the components. Frequently they are su-
perficial ooids, with spherical to ovoidal shapes. Type I
oncoids, peloids and intraclasts are occasional.

This facies corresponds to higher energy environ-
ments compared to the previously described facies 2
and 3. Micritic ooids would be formed in the shoal en-
vironment, under the continuous agitation of the sea
floor (Strasser, 1986). The existence of fragments of
corals and stromatoporoids floating in the oolitic sedi-
ment indicates the proximity of coral reefs to the shoal
environment.

4.6. Facies 5: Oolitic packstone-grainstone with Marinella

Facies 5 is arranged in irregular beds (up to 0.4 m
thick) with local planar cross-bedding. The facies is char-
acterized by the presence of fragments of the red algae
Marinella lugeoni and spherical to ovoid type 3 and type

4 ooids (Fig. 7a). The nuclei of these ooids are miliolids,
lituolids, algae, echinoderms and quartz grains. Besides
the red algae *Marinella*, the main skeletal components
are gastropods and bivalves. Foraminifera (miliolids, tex-
tularids and lituolids), *Cayeuxia*, echinoderms and sole-
noporacean are less abundant. Peloids and aggregates are
also occasionally found. Type II oncoids and intraclasts
(fragments of peloidal and burrowed bioclastic inter-reef
facies) are also present.

Similar facies showing *Marinella* bioclasts associated
with oolites were described in the Portuguese Upper
Jurassic (Leinfelder *et al.*, 1996). These were formed in
high-energy settings, where the algae *Marinella* had the
ability of regenerate from broken fragments. *Marinella*
was able to colonize environments that were not previ-
ously occupied by other encrusting organisms such as mi-
crobial forms, *Bacinella* or *Lithocodium*. The facies can
be divided into two textural groups, according to the ma-
trix proportion, indicating a progressive energy increase
from relatively distal wackestone-packstone to proximal
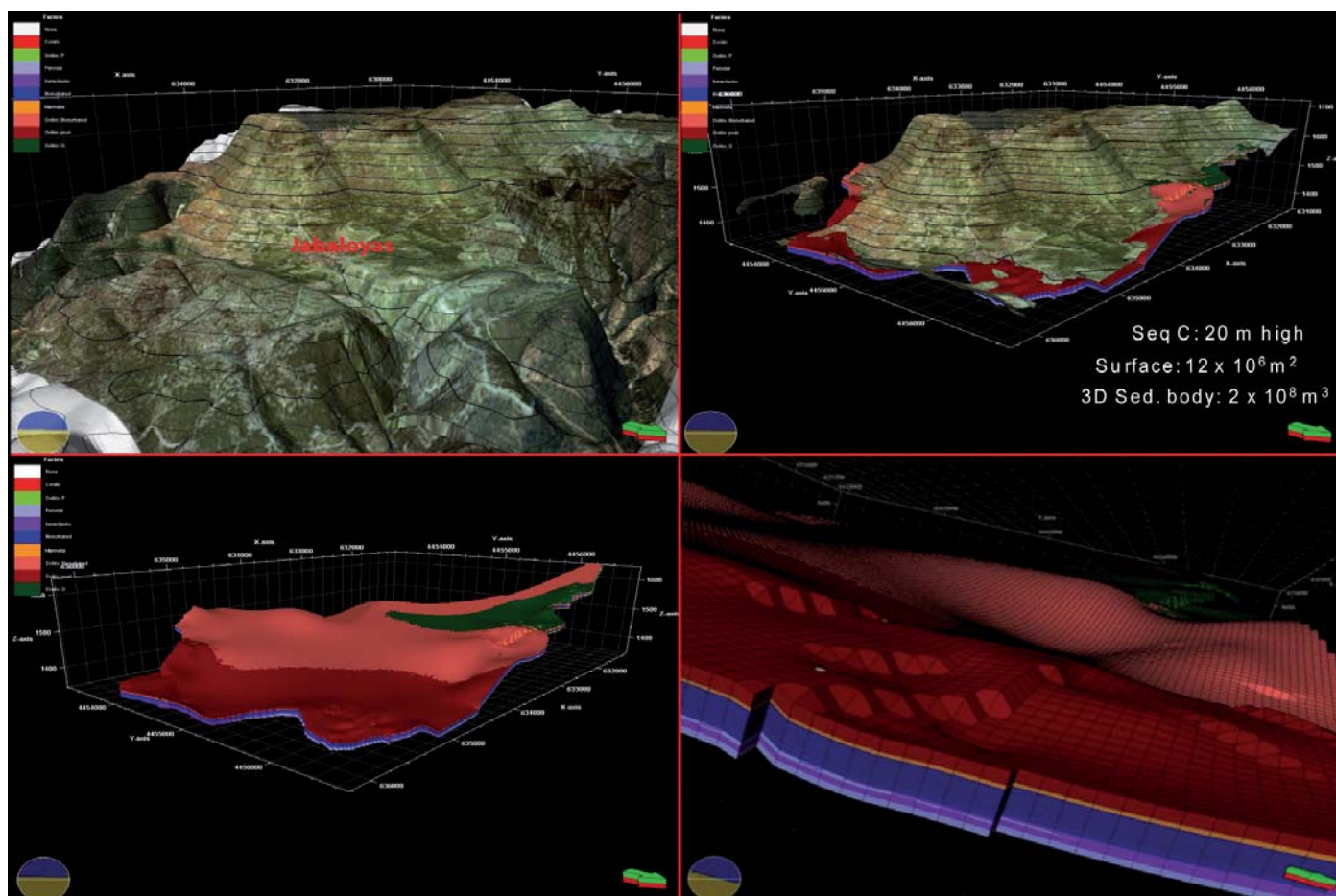packstone-grainstone textures.

Fig. 13.- Pictures exported from the 3D model that measured 12 km^2 and 3x10^8 m^3 (vertical scale is exaggerated x5). On the right bottom picture, the grid increment of the Full-field Model can be observed (20 x 20 m), that better fit with the facies belts of the carbonate ramp. The layering was adjusted to the beds of each episode (between 0.2 and 0.5 m thick).

Fig. 13.- Fotografías exportadas del modelo 3D. Mide 12 km^2 y 3x10^8 m^3 (la escala vertical está exagerada x5). El incremento de la malla del modelo de campo completo es de 20 m, el cual representa mejor la geometría de los diferentes cinturones de facies. Las capas fueron ajustadas para cada estadio evolutivo (variando desde 0,2 a 0,5 m).

4.7. Facies 6: Burrowed peloidal-oolitic wackestone-packstone

The facies is arranged in tabular beds up to 1.3 m thick. The main components are ovoid and irregular peloids (up to 70% of the components) up to 0.4 mm in diameter (Fig. 7e,f). Ovoid and spherical type 3 and 4 ooids up to 1 mm in diameter form up to 40% of the components. The main bioclasts (up to 20%) are foraminifera (miliolids, *Nautiloculina oolithica*, lituolids, including *Alveosepta jaccardi*) and gastropods. Bivalves, other benthic foraminifera (textularids) and *Marinella lugeoni* are occasionally found. Type II oncoids are present in lower proportion. The presence of muddy textures and peloids reflect low-energy depositional environments probably located in the back side of the active shoal.

In contrast with the previously described facies 1 to 5, facies 6 was deposited after the coral-microbial reef buildups growth (i.e., post-reef facies). The post-reefal

character of the facies is indicated by the absence of bioclasts of colonial organisms and by its onlapping geometry over the reefs (Fig. 4 and 8f). Hence, the decrease of the energy can be explained by the "barrier" formed by the oolitic-bioclastic shoals (in combination with the C2 reef palaeo-relief; see section 5). The presence of *Alveosepta jaccardi* (Lituoloidea superfamily, Fig. 7f) highlights the deposition of this facies in the shallow inner ramp setting (Flügel, 2004).

4.8. Facies 7: Oolitic-peloidal packstone-grainstone

The facies is arranged in irregular beds up to 0.6 m thick with planar cross-lamination (Fig. 7c). It shows up to 50% of ovoidal, sub-spherical and spherical fibrous-radial type 3 and type 4 ooids, up to 1 mm in diameter (Fig. 7d). Peloids (up to 45% of the components) are irregular, ovoid and spherical and no larger than 0.4 mm in diameter. Bioclasts are dominated by bivalves and
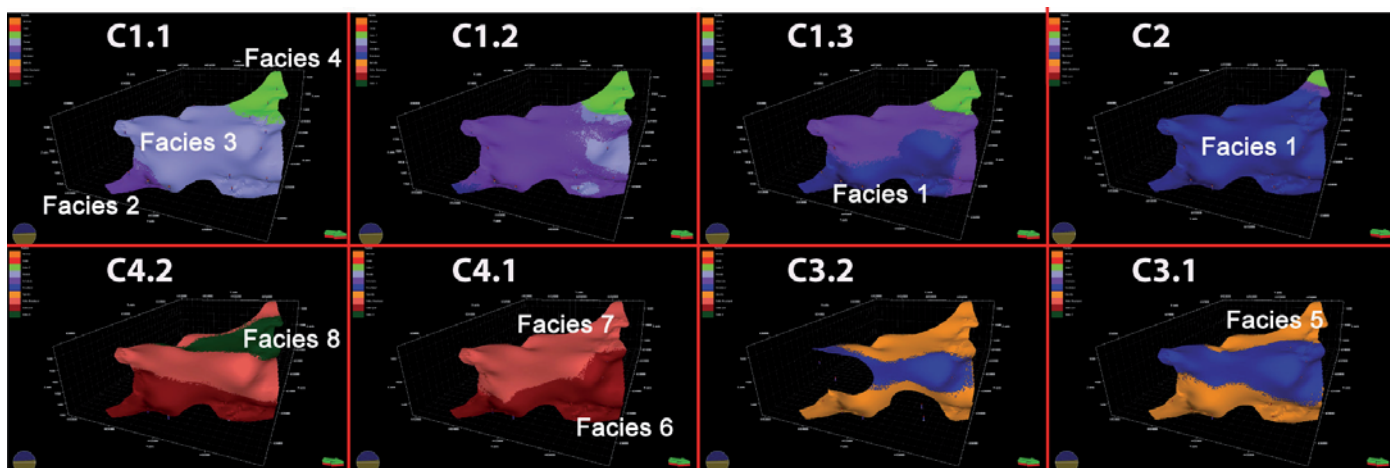
Fig. 14.- Video slides from the Full-field Model showing the adjustment to the interpreted facies maps.
Fig. 14.- Fotogramas de capas seleccionadas del modelo de campo completo que muestra el ajuste realizado con respecto a los mapas de facies.
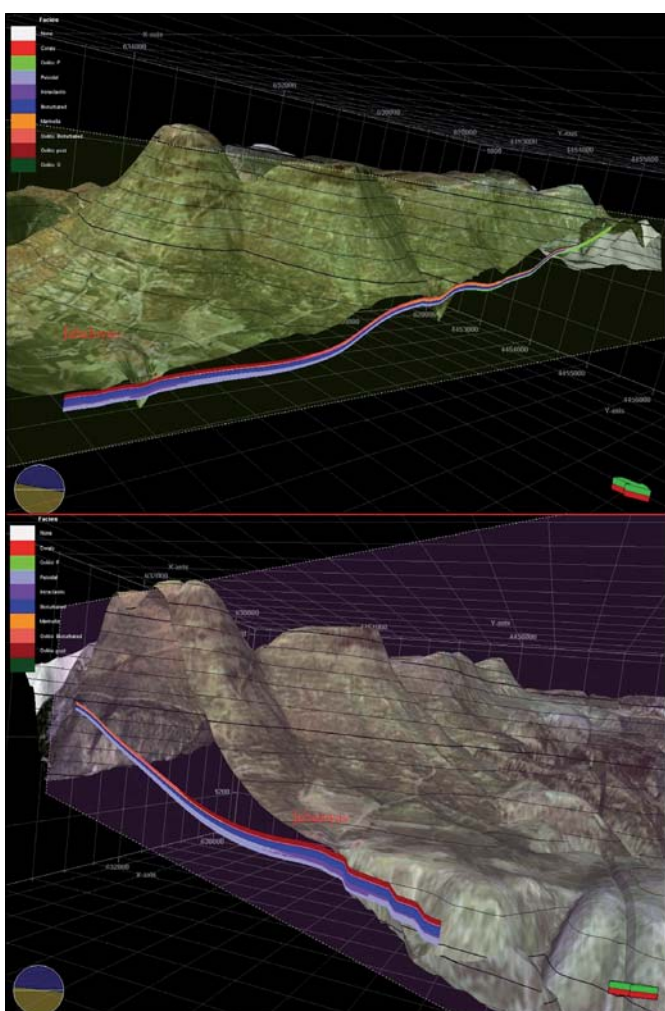

Fig. 15.- Transversal cross-sections taken from the Full-field Model. The general appearance of the basinward thickening of the sequence is visible on the picture at the top. Close to Jabaloyas village the sequence C exhibits the dominance of the mud-dominated facies (dark colour).
Fig. 15.- Cortes geológicos del modelo de campo completo. Se aprecia el aspecto general de la secuencia con un incremento en su espesor conforme no acercamos a zonas mas distales. En las cercanías de Jabaloyas, predomina la facies 5 no granosostenida (color oscuro).

foraminifera (miliolids, lituolids, *Lenticulina*, textularids). Gastropods, echinoderms, *Marinella lugeoni* and *Cayeuxia* occasionally occur. Type II oncoids, aggregate grains, compound ooids and quartz grains are occasionally found.

The existence of type 4 ooids and planar cross-lamination and the abundance of bivalves and foraminifera indicate deposition during episodic high-energy events in a non-restricted interior lagoon.

4.9. Facies 8: Oolitic grainstone

Facies 8 consists of tabular beds (up to 0.5 m thick) with frequent planar cross-bedding (Fig. 8e). The ooids (95% of the components) are spherical, up to 1.5 mm in diameter (Fig. 7b). Type 3 and type 4 ooids are found in larger proportion than high-energy type 1 ooids. Gastropods and foraminifera (miliolids and lituolids) are often found, most of them surrounded by incipient oolitic coatings. The bioclasts are mainly bivalves. Quartz grains are observed in low proportion, forming the nuclei of the ooids.

Facies 8 represents an oolitic sand bar formed in very shallow domains (i.e., the shoreface) which occurred parallel to the shoreline. Palaeocurrent measurements indicate a longshore driven current (i.e., SW-NE).

5. Facies distribution and sedimentary model

Extensive fieldwork and facies analysis, including lateral tracing of some key surfaces, analysis from photomosaics and detailed logging, resulted in a precise understanding of the lateral and vertical distribution of coral reefs and associated inter- and post-reef facies that have been described above. The information is summarized in figure 9, showing the correlation between the 17 logged
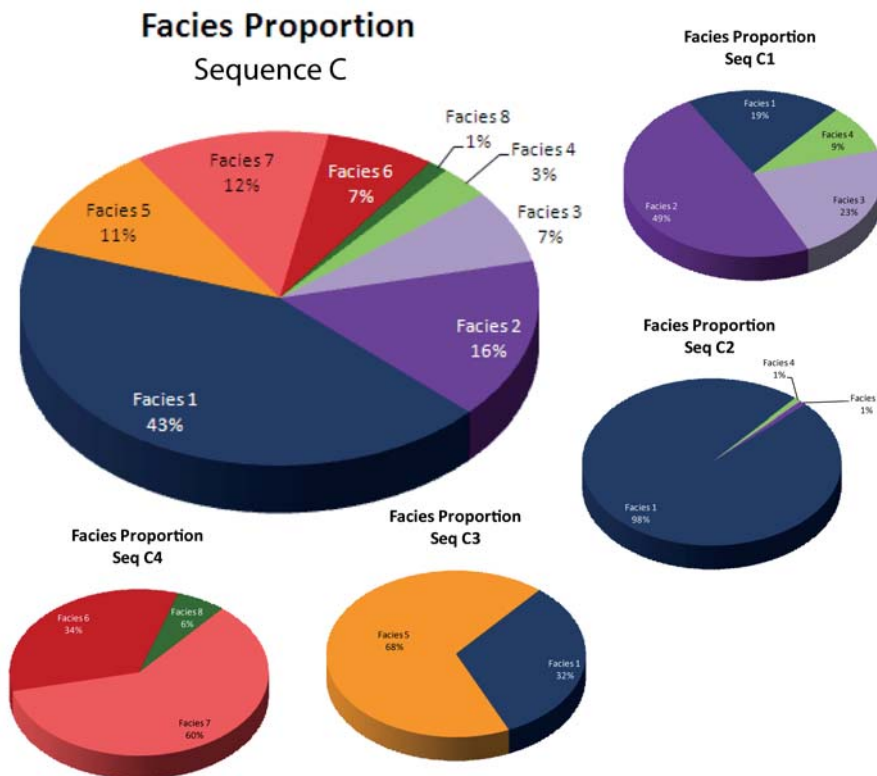
Fig. 16.- Relative facies proportions based on volume calculation in each episode. Once the Full field Model has been created, the volume calculation was automatically obtained for three dimensional bodies that can be split by assigning sedimentological properties.
Fig. 16.- Proporción relativa de las facies en el modelo total y separada por estadios evolutivos. Una vez creado el modelo 3D, la separación y cálculo de volúmenes de cuerpos por propiedades es automática.

profiles. The northern and southern correlation panels show the facies distribution from proximal to distal ramp areas, whereas the eastern correlation panel would be almost parallel to the defined facies belts. These panels also show the progressive thickness increase of the studied high-frequency Sequence C from proximal to distal localities, reaching up to 20 m in more distal stratigraphic profiles (BB). The studied Sequence C is bounded by planar and well-cemented discontinuity surfaces that can be traced at regional scale (see Aurell and Bádenas, 2004; and Bádenas and Aurell, 2010, for details).

The sequence displays a deepening-shallowing upward trend, and was described by Aurell and Bádenas (2004) as a catch-down type sequence (nomenclature according to Hillgärtner and Strasser, 2003). Four sedimentary episodes have been established within Sequence C, named C1, C2, C3 and C4 episodes. They are bounded by discontinuity surfaces (i.e., sharp burrowed and ferruginous bedding planes), linked to abrupt vertical facies changes (see Fig. 9).

The performed sedimentological analysis allows a precise reconstruction of the different facies belts in the low angle carbonate ramp where the facies of the studied Upper Kimmeridgian high-frequence sequence were deposited. There are no clear evidences pointing to the deposition in intertidal environments. All the described facies have been interpreted as deposited in subtidal environments, in an almost pure carbonate system. The siliciclastic input in Sequence C is very low and sand-size quartz grains are mostly found as nuclei of the different types of ooids, mostly in episodes C3 and C4. Occasional quartz concentrations in distal facies were possibly caused by storm-induced density flows.

As it is indicated by the reconstructed lateral and vertical facies distribution (see Fig. 9), there is a progressive transition from proximal facies 6 to 8 deposited in the protected interior ramp areas (i.e., back barrier lagoon) to relatively open marine domains (i.e., proximal middle ramp) represented by the mud-dominated facies 1. The observed relationship between the coral-microbial buildups and the coeval inter-reef facies 1 to 4 shows that the development of the buildups occurred mostly in the midramp domain. Some smaller size patches or biostromes have been observed during the episode C3, time-equivalent of the *Marinella* facies 5.

The reconstructed sedimentary model illustrated in figure 10 shows the distribution of coral reef facies and inter- and post-reef facies 1 to 8. This is an idealized model, because any of the four episodes C1 to C4 includes all the facies: episodes C1 and C2 encompass facies 1 to 4; episode C3 is formed by facies 1 and 5, and episode C4 only includes the more proximal facies 6 to 8. The relative proportion of the key components found in the different facies types is indicated in figure 11, showing the down-dip gradation of the different non-skeletal grains. The extent of the coral-microbial reefs across the ramp during episodes C1 and C2 is also shown.
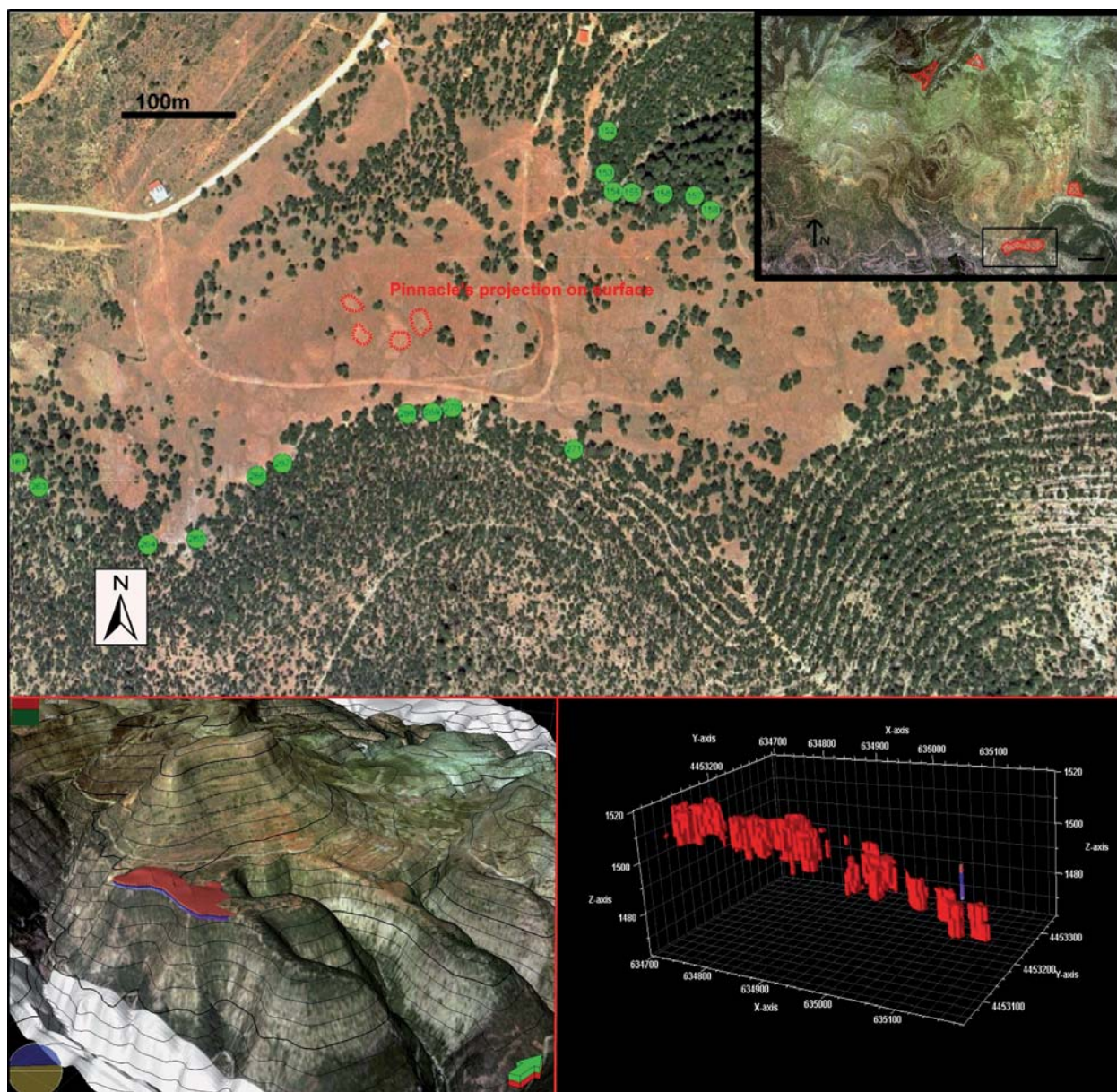
Fig. 17.- Aerial view of the selected area for the Sector Model, a structural platform that cut the top of Sequence C: The reef bodies appearing as circular-elliptical spots. These spots are compatible with reef fabric in the field and they were used as a template for the object modelling in the Sector Model (red objects at the bottom of the figure).

Fig. 17.- Vista aérea de la zona seleccionada para realizar el modelo sector, una plataforma estructural donde la secuencia se ve cortada hacia su parte más alta y los pináculos aparecen formando manchas con geometrías circulares y elípticas. Estas manchas son correlacionadas en campo con fábrica arrecifal y fueron usadas como plantilla para la modelización de los arrecifes en el modelo sector (objetos rojos en la figura de la esquina izquierda).

6. Sedimentary evolution

The four episodes C1–C4 document the sedimentary evolution of the Sequence C (see in figure 12 successive facies distribution maps for each episode). Episode C1 represents the Transgressive Deposits (TD) of the studied Sequence C, as indicated by the retrogradation of the low-energy distal facies 1 until the maximum flooding surface (mfs, green dashed line in Fig. 9). This mfs is a borrowed and ferruginized surface, which coincides in proximal areas with a sharp vertical facies change from grain-supported to mud-supported facies (S2 surface in Aurell and Bádenas, 2004; see S2 in Fig. 9). Additionally, this surface correlates with a condensed surface within the buildups, which is followed by a thin level where microbial crusts predominate over the colonial organisms.

The episode C2 is interpreted as the early Highstand Deposits (HD) and is dominated by the sedimentation of the low-energy mud-supported facies 1 through the most part of the study area. The deposition of low-energy

facies occurred in response to the relative high sea level. A sharp surface associated with a sudden facies change that can be traced across most of the study area separates the C2 and C3 episodes (see Fig. 9).

Regarding the main components of the lower episodes C1 and C2, type 1 ooids dominated in more proximal areas, passing gradually basinwards into peloidal-intraclastic facies (Fig. 11). The reef-derived debris (peloids and intraclasts) and skeletal grains (colonial organisms, solenoporacean algae) are widespread over all the studied domains, coeval to the growing of coral-microbial reefs. The reefs grew from high-energy to low-energy mid-ramp areas, mostly during the episodes of rapid gain of accommodation. The presence of bivalves, echinoderms and serpulids tends to increase towards relatively deep waters. Benthic foraminifera locally appear close to the active shoal environment probably as resedimented particles.

The upper two episodes C3 and C4 correspond to the late HD of the Sequence C, defined by a rapid facies progradation (Fig. 9). Episode C3 is characterized by the progressive onlap of facies 5 (which was filled by *Marinella*-oolitic facies) over the top of the reef pinnacles, involving the eventual filling of the irregular topography left by the reef palaeohighs at the sea floor. In addition, facies 5 does not include significant amount of reef debris, indicating that the coral-microbial reefs were not productive when facies 5 was deposited. The proximity of inner ramp domains is outlined by the abundance of sparitic ooids and benthic foraminifera. However, the *Marinella*-rich facies were deposited in open environments, as indicated by the gradual change to the offshore mud-supported facies 1. It is remarkable that there was also a direction change of the facies belts from episodes C1 and C2 to episode C3 (from NE-SW to N-S; Fig. 12).

The uppermost episode C4 is characterized by the widespread deposition in backshoal environment, that is the widespread progradation of the inner ramp facies 6 to 8. Facies 6 represents relatively low-energy environments behind the active shoal with high proportion of lime mud. These conditions allowed the formation of larger type 4 ooids, dominating over the other types in these backshoal areas. The characteristic massive bioturbated beds of facies 6 also contain high amount of benthic foraminifera and the proportion of bioclasts from *Marinella* algae has been considerably decreased. Resedimented ooids from the active shoals are also present in this facies. Peloids could be formed by micritization processes in these low agitation environments. Gastropods and miliolid foraminifers are common in this low-energy, back barrier depositional setting. The presence of the ooid-rich facies 7 and 8 found at the top of the sequence marks the last episode with the progradation of the ooid sand bar. The sand bars represented by facies 7 and 8 are almost completely composed by type 3 and type 4 ooids.

7. 3D Modelling

Two 3D models of the vertical and lateral facies distribution around the Jabaloyas area have been built using Petrel software: the complete modelling of the study area around Jabaloyas or Full-field Model and a more specific area close to the BH stratigraphic profile (i.e., the Sector Model), in order to draw in detail the relationship between the coral-microbial reefs and the inter-reef facies.

7.1. Full-field Model

Studying the distribution and the geometries of the main sedimentological bodies within the Sequence C has provided an adequate amount of information to create a 3D Full-field Model, with a size of 12 km^2 and 2 x 10^8 m^3. Exported pictures from the model have been added in figure 13. The selected grid increment for this model was 20 x 20 m.

The cemented bed found at the top of the studied interval was used as reference surface in the 3D modelling. The key-bounding surfaces between the episodes defined in Sequence C were also incorporated in the 3D model. These surfaces were adjusted to some minor fault planes which were not incorporated as 3D objects. The Facies modelling was carried out with the Truncated Gaussian algorithm with trends. The facies maps reconstructed from the field data were adjusted layer by layer during the performed simulation. The resulted facies belts that have been reconstructed from field observations are approximately 1–3 km width (Fig. 12).

The exported pictures of the Full-field Model in figure 14 and the cross-sections in figure 15 show the adjustments of the modelled facies distribution to the facies maps and correlation panels respectively, which were interpreted directly from the stratigraphic profiles. Regarding the E-W cross-section (Fig. 15, above), it would correspond to the northern section where it encompasses the most important lateral facies change from proximal to distal areas (see Fig. 9). The N-S cross-section reproduced in figure 15 (below) was adjusted to the eastern section (see Fig. 9), where the muddy facies 1 dominates.

The relative proportion of each facies for each episode and the total proportion for the whole Sequence C is given in figure 16. Facies 1 represents the major sedimentary body with a total volume of 8.55 x 10^7 m^3 (few cubic metres in C1 and C3 but 6.32 x 10^7 m^3 in C2). Facies 4, located only in proximal areas, represents a body of

6.31×10^6 m^3. The other facies form sedimentary bodies between $1-3 \times 10^7$ m^3, excepting the ooid sand bar (facies 8) that only has 2.51×10^6 m^3. Similar workflow with petrophysical properties could be also interesting for simulation purposes by assigning mainly porosity and permeability data into the different facies types.

7.2. Sector Model

The Sector Model was necessary to incorporate the reef bodies in the 3D model. The selected area represents a 0.12 km^2 surface on a modern structural platform where the Sequence C is weathered at a certain height. It entails the visualization of the real geometry of the individual boundstone buildups in the aerial picture (Fig. 17). The Object Modelling was adjusted to these spots. The selected Sector Model grid increment was 0.5×0.5 m and its 3D building was created based on the same limiting surfaces from the Full-field Model. The total volume of the sector model is 1×10^7 m^3.

The coral-microbial reefs of the area selected for the Sector Model are located between the BH and BS2 logs and correspond to the relatively distal ramp domains (see Fig. 9 and 12). The buildups have a relatively low spatial density, forming isolated pinnacle bodies up to 19 m thick. Reef buildups have the spherical and elliptical geometries that could be seen from aerial view (see "pinnacle projection in surface" in the upper part of Fig. 17).

8. Conclusion and perspectives

The 3D reconstruction of the facies heterogeneities within a high-frequency sequence (Sequence C, 12 to 20 m thick) has been carried out. This sequence encompasses the inner to middle facies of the Late Kimmeridgian carbonate ramp. Facies analysis allowed the definition of eight facies from proximal to distal settings, with different proportion of skeletal and non-skeletal components (ooids, peloids, intraclasts and oncoids). Based on the facies distribution, the studied sequence was further divided into four episodes. The lower episodes (C1, C2) correspond to the development of mud to grain-supported mid-ramp facies (intraclastic, skeletal, peloidal, oolitic) and coral-microbial reefs. The upper episodes (C3, C4) cover the rapid progradation of proximal facies. Episode C3 is characterized by the widespread presence of the red algae *Marinella lugeoni*, which marks the transition area between the higher energy inner ramp and the mid-ramp domain.

The studied outcrops allowed the identification and georeferencing of 274 coral-microbial buildups, showing conical to pinnacle cylindrical geometry up to 19 m thick. These buildups accumulated during the main episodes of accommodation gain, corresponding to the transgressive and early highstand stages of Sequence C (i.e., episodes C1, C2). Most of coral-microbial reef growth occurred in the mid-ramp. Towards the inner-middle ramp transition, local amalgamations and eventual development of reef ribbons up to 50 m long are observed.

The quality of Jabaloyas outcrops provides precise data for the creation of 3D models. Two models were developed: a Full-field Model allowing calculation of volume and proportion of inter-reef and post-reef facies; and a Sector Model, where the reef bodies were incorporated. These models have been used as a template for further test on diagenesis overprint and resulting distribution of reservoir bodies and connectivity for sector simulation (phenomenology purposes) with real reservoir/field data. The precise reconstruction of reefal and inter-reef facies might be used as a template for further tests on diagenesis. For this purpose, integrated analysis within different techniques (Electromagnetic multifrequency broadband survey and Magnetometry) and Ground Penetrating Radar resolutions has exhibited a potential approach to develop a high-resolution 3D reconstruction of pinnacles. Preliminary results have been published in Pueyo-Anchuela *et al.* (2011).

References

Al-Saad, H., Ibrahim, M., (2005): Facies and palynofacies characteristics of the Upper Jurassic Arab D reservoir in Qatar. *Revue de Paléobiologie* 24 (1), 225-241.

Aurell, M., Robles, S., Bádenas, B., Quesada, S., Rosales, I., Meléndez, G., García-Ramos, J.C., (2003): Transgressive/Regressive Cycles and Jurassic palaeogeography of NE Iberia. *Sedimentary Geology* 162, 239-271. doi: 10.1016/S0037-0738(03)00154-4.

Aurell, M., Bádenas, B., (2004): Facies and depositional sequence evolution controlled by high-frequency sea-level changes in shallow-water carbonate ramp (late Kimmeridgian, NE Spain). *Geological Magazine* 141 (6), 717-733. doi: 10.1017/S0016756804009963.

Aurell, M., Ipas, J., Bádenas, B., Muñoz, A., (2011): Distribución de facies con corales y estromatopóridos en el dominio interno de una plataforma carbonatada (Titónico, Cordillera Ibérica). *Geogaceta* 51, 67-70.

Ayoub, R., En Nadi, I. M., (2000): Stratigraphic framework and reservoir development of the Upper Jurassic in Abu Dhabi area, U.A.E. In: Abdulrahman, Alsharhan, S., Scott R. W., *Middle East Models of Jurassic/Cretaceous Carbonate System* Vol. 69, 229-248.

Bádenas, B., Aurell, M., (2001): Kimmeridgian palaeogeography and basin evolution of northeastern Iberia. *Palaeogeography, Palaeoclimatology, Palaeoecology* 168, 291-310. doi: 10.1016/S0031-0182(01)00204-8.

Bádenas,B., Aurell, M., (2010): Facies models of a shallow-water carbonate ramp based on distribution of non-skeletal grains (Kimmeridgian, Spain). *Facies* 56, 89-110. doi: 10.1007/s10347-009-0199-z.

BP Statistical Review of World Energy. June 2011.

Dahanayake, K., (1977): Classification of oncoids from the Upper Jurassic carbonates of the French Jura. *Sedimentary Geology* 18, 337-353. doi: 10.1016/0037-0738(77)90058-6.

Dahanayake, K., (1978): Sequential position and environmental significance of different types of oncoids. *Sedimentary Geology* 20, 301-316. doi: http://dx.doi.org/10.1016/0037-0738(78)90060-X.

Dunham, R.J., (1962): *Classification of carbonate rocks according to depositional texture.* American Association Petroleum Geology Memoir 1, 108-121..

Embry, A. F., Klovan, J. E., (1971): A late Devonian reef tract on northeastern Banls Island, Northwest Territories. *Bulletin Canadian Petroleum Geology* 19, 730-781.

Fezer, R., (1988): Die Oberjurassische Karbonatische Regressionsfazies im sudwestlichen Keltiberikum zwischen Griegos und Aras de Alpuente (Prov. Teruel, Cuenca, Valencia, Spanien). Arb. Inst. Geol. Palaont. Univ. Stuttgart. 84, 1-119.

Flügel, E. (2004): *Microfacies of Carbonate Rocks. Analysis, Interpretation and Application*. Springer. 976 p.

Grötsch, J., Suwaina, O., Ajlani, G., Taher, A., El-Khassawneh, R., Lokier, S., Coy, G., van der Weerd, E., Masalmeh, S., van Dorp, J., (2003): The Arab Formation in central Abu Dhabi: 3-D reservoir architecture and static and dynamic modelling. *GeoArabia*, Vol. 8, No. 1, Gulf PetroLink, Bahrain.

Hillgärtner, H., Strasser, A., (2003): Quantification of high-frequency sealevel fluctuations in shallow-water carbonates: an example from the Berriasian–Valanginian (French Jura). *Palaeogeography, Palaeoclimatology, Palaeoecology* 200, 43–63. doi: 10.1016/S0031-0182(03)00444-9.

Jahn, F., Cook, M., Graham, M., (2003): Hydrocarbon exploration and production. Elsevier. TRACS International Consultancy Ltd. Aberdeen, UK.

Jennings, J.W., (2000): Spatial statistics of permeability data from carbonate outcrops of West Texas and New Mexico: Implications for improved reservoir modeling. The *Report of Investigations*. University of Texas at Austin, Bureau of Economic Geology, No. 258, 50 p.

Lehmann, C. T., Ibrahim, K., Bu-Hindi, H., Al-Kassawneh, R., Cobb, D., Al-Hendi, A., (2008): High-Resolution Sequence Stratigraphic Interpretation of the Upper Jurassic Arab Formation from New Field Development, Offshore Abu Dhabi. Search and Discovery Article Adapted from oral presentation at AAPG Annual Convention, San Antonio, Texas, April. 20-23.

Leinfelder, R.R, (1993): Upper Jurassic types and controlling factors. *Profil* 5, 1-45.

Leinfelder, R. R., Werner, W., (1993): Systematic position and palaeoecology of the Upper Jurassic to Tertiary alga Marinella lugeoni Pfender. *Zitteliana* 20, 105-122.

Leinfelder, R.R., Werner, W., Nose, M., Schmid, D.U., Krautter, M., Laternser, R., Takacs, M., Hartmann, D., (1996): Palaeoecology, Growth Parameters and Dynamics of Coral, Sponge and Microbolite Reefs from the Late Jurassic. In: Reitner, J., Neuweiler, F. & Gunkel, F. (Eds.): Global and Regional Controls on Biogenic Sedimentation. I. Reef Evolution. Research Reports. *Göttinger Arb. Geol. Paläont.* Sb2, 227-248.

Leinfelder, R. R., Schlagintweit, F., Werner, W., Ebli, O., Nose, M., Schmid, D., Hughes, G. W., (2005): Significance of stromatoporoids in Jurassic reefs and carbonate platforms – concepts and implications. *Facies* 51, 287 – 325. doi: 10.1007/s10347-005-0055-8

Nose, M., (1995): Vergleichende Faziesanalyse und Palökologie korallenreicher VerXachungsabfolgen des Iberischen Oberjura. *ProWl* 8, 1–237.

Pueyo-Anchuela, Ó., San Miguel, G., Martínez, V., Aurell, M., Bádenas, B., (2011): Discriminación potencial de facies arrecifales por métodos geofísicos: aplicación a los pináculos arrecifales del Kimmeridgiense de Jabaloyas (Teruel). *Geogaceta* 51, 95-98.

Schlumberger Limited, (2011): Petrel 2010.2 E&P Software Platform® (access: 16/01/2013. http://www.slb.com/services/software/geo/petrel.aspx)

Strasser, A., (1986): Ooids in Purbeck limestones (Lowermost Cretaceous) of the Swiss and French Jura. *Sedimentology* 33, 711-727. doi: 10.1111/j.1365-091.1986.tb01971.x.